analytical chemistry
Article
pubs.acs.org/ac

Laser-Induced Acoustic Desorption of Natural and Functionalized Biochromophores

Uğur Sezer,[†] Lisa Wörner,[†] Johannes Horak,[†] Lukas Felix,[‡] Jens Tüxen,[‡] Christoph Götz,[§] Alipasha Vaziri,[§] Marcel Mayor,[‡,∥] and Markus Arndt*[,†]

[†]University of Vienna, Faculty of Physics, VCQ and QuNaBioS, Boltzmanngasse 5, 1090 Vienna, Austria
[‡]University of Basel, Department of Chemistry, St. Johannsring 19, 4056 Basel, Switzerland
[§]University of Vienna, Max F. Perutz Laboratories, Research Institute of Molecular Pathology, QuNaBioS, Doktor-Bohr-Gasse 7, 1030 Vienna, Austria
[∥]Karlsruhe Institute of Technology (KIT), Institute of Nanotechnology, P.O. Box 3640, 76021 Karlsruhe, Germany

Supporting Information

ABSTRACT: Laser-induced acoustic desorption (LIAD) has recently been established as a tool for analytical chemistry. It is capable of launching intact, neutral, or low charged molecules into a high vacuum environment. This makes it ideally suited to mass spectrometry. LIAD can be used with fragile biomolecules and very massive compounds alike. Here, we apply LIAD time-of-flight mass spectrometry (TOF-MS) to the natural biochromophores chlorophyll, hemin, bilirubin, and biliverdin and to high mass fluoroalkyl-functionalized porphyrins. We characterize the variation in the molecular fragmentation patterns as a function of the desorption and the VUV postionization laser intensity. We find that LIAD can produce molecular beams an order of magnitude slower than matrix-assisted laser desorption (MALD), although this depends on the substrate material. Using titanium foils we observe a most probable velocity of 20 m/s for functionalized molecules with a mass m = 10 000 Da.

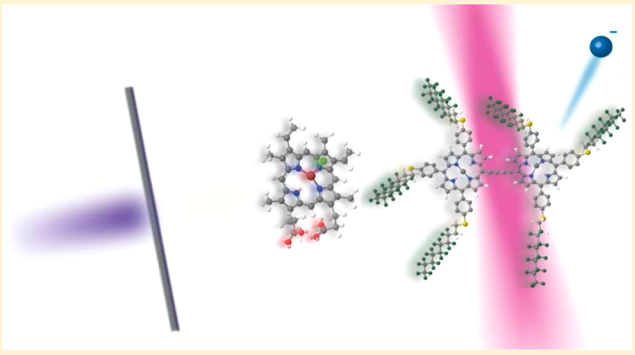

Many analytical chemistry studies have focused on how to launch and control charged molecules, for instance using matrix-assisted laser desorption ionization (MALDI)[1] or electrospray ionization (ESI).[2] However, it is of analytical relevance to revisit methods that are capable of transferring neutral or lowly charged molecules into the gas phase, free from any carrier gas or matrix. LIAD[3] is a method that avoids these contaminants and allows analytes to be launched into a high vacuum environment, for example, close to the ionization region of a TOF-MS. It minimizes transfer losses between the source and the mass analyzer with the potential to detect rare samples very efficiently. In contrast to MALDI and ESI, LIAD separates the launch and the ionization mechanism. This enables particle specific detection through multiphoton ionization.

In a typical LIAD experiment the analyte molecules are placed on the front side of a metal foil that is several micrometers thick. A short, intense laser pulse incident on the back side ablates some foil material. Shock waves induced by thermo-mechanical stress in the foil[4,5] eject analyte molecules and substrate material from the front side.

LIAD was originally used to launch electrons and ions[3] and soon after it was extended to large polypeptides[6] and even DNA strands.[7] It has also been used to load neutral or lowly charged medium-sized molecules into mass spectrometers[8] and even to launch silicon nanoparticles[9] or biological cells[10] up to a mass of 10^{10} Da.

Here, we extend the application of LIAD to biochromophores, study the softness of this technique, and the effect of molecular functionalization on the desorption process. In addition, we investigate the velocity of the desorbed molecules and find that even for these very large particles the velocity is significantly lower than in MALDI. This will be beneficial for analytical chemistry, physical chemistry, spectroscopy, ionization studies,[11,12] classical beam deflectometry,[13−15] molecular cooling,[16] and matter-wave experiments.[17,18]

EXPERIMENTAL SECTION

Molecules. Hemin, bilirubin, biliverdin, and zinc tetraphenylporphyrine (ZnTPP) were obtained commercially from Sigma-Aldrich. The chlorophyll a was extracted and purified from spinach in ethanol following an established procedure.[19] ZnTPP was dissolved in acetone, while all other molecules were dissolved in dimethyl sulfoxide (99.9%) with a concentration of

Received: February 12, 2015
Accepted: May 6, 2015
Published: May 6, 2015

DOI: 10.1021/acs.analchem.5b00601
Anal. Chem. 2015, 87, 5614−5619

10 mg/mL. An array of small droplets (~2 μL) of this solution was deposited onto a clean, thin titanium foil with a thickness of 10 ± 2 μm and a purity of 99%. The sample was then transferred into the vacuum chamber.

To explore how perfluoroalkyl-functionalization can facilitate the desorption process, we synthesized two sets of molecules (see the Supporting Information). The diporphyrin **1*Lx***, shown in Figure 1a, is a molecular library that covers a mass range of

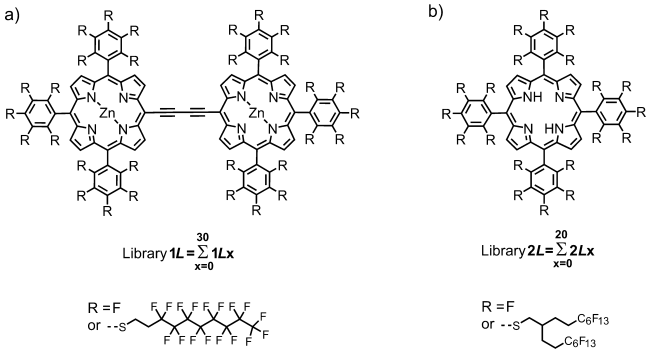

Figure 1. Perfluoroalkylated porphyrins for desorption studies with LIAD. In panel a the diporphyrin library **1*Lx*** is displayed. Each of the fluorine atoms on the outer phenyl rings can be substituted with a perfluoroalkyl chain. In panel b the structure of the porphyrin library **2*Lx*** is sketched. To achieve higher molecular masses, a number x of branched alkyl side chains have been used.

3 630−5 470 Da in steps of 460 Da. It can be synthesized from two porphyrin building blocks in a single step using a Glaser-Hay coupling.[20,21] All substituents of the phenyl rings in the porphyrin meso positions are either fluorine atoms or perfluoroalkylsulfanyl groups. Figure 1b shows our second molecular library **2*Lx*** which covers masses beyond 10 000 Da.[22,23]

The perfluoroalkylated molecules were prepared in diethyl ether and dried on a pure tantalum foil as this was found to increase the number of detected particles. The addition of 2 mg/mL of 2,5-dihydroxybenzoic acid (DHB) to the solution of **2*Lx*** also increased the signal. In contrast to MALDI, where DHB fosters molecular ionization, we detect no ions originating from the LIAD process without the postionization stage.

Experimental Setup. Figure 2 shows a drawing of the experimental setup. A motorized manipulation stage positioned the foil targets at a distance D = 23 ± 1 mm to the detection laser beam when using the natural chromophores and at D = 43 ± 2 mm otherwise. The light of a frequency tripled Nd:YAG laser was focused to a waist of 1 mm diameter on the back side of the metal foil. In order to expose a fresh sample spot to every desorption laser pulse, the stage was translated laterally. The neutral molecules fly into the extraction region of the TOF-MS where they intersect a 157.6 nm fluorine-laser beam which ionizes them.

RESULTS: BIOCHROMOPHORES

Mass Spectra. Figure 3 shows typical LIAD mass spectra of all four biochromophores at comparable photoionization laser intensities. Each spectrum is an average over 30 shots.

Figure 3a shows the hemin mass spectrum $[\text{Fe Por-Cl}]^+$ at m = 652 Da as well as $[\text{Fe Por}]^+$ and further peaks attributed to the loss of CH_2COOH-groups. Chlorophyll is a derivative of hemin, and its core survives the LIAD process undamaged. We observe a peak at 871 Da, corresponding to pheophytin a, i.e.,

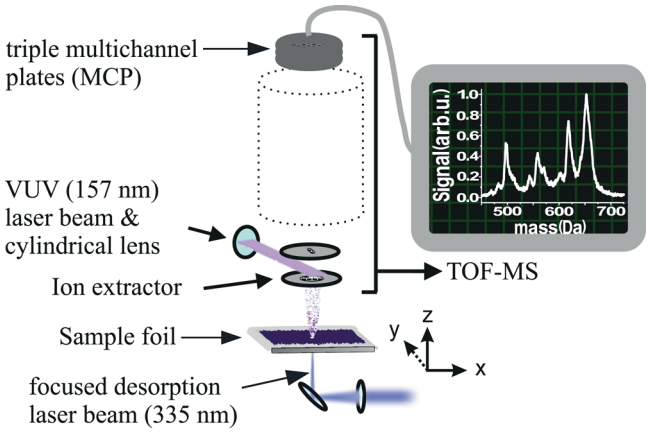

Figure 2. Molecules are volatilized by laser-induced acoustic desorption from the front surface of a thin metal foil by irradiating its backside with intense pulsed laser light with λ_{des} = 355 nm, τ_{des} = 4 ns, Φ_{des} = 10−510 MW/cm^2. The emerging plume is postionized using vacuum ultraviolet light, with λ_{ion} = 157.6 nm, τ_{ion} = 8 ns, Φ_{ion} = 0.16−2.2 MW/cm^2, and characterized using TOF-MS.

the intact parent molecule without the central magnesium atom. However, we also find a fragment signal at 536 Da which is attributed to pyropheophorbide a. LIAD is also capable of generating beams of intact neutral bilirubin (Figure 3c) and biliverdin (Figure 3d). Bilirubin exhibits additional fragments at 286 and 300 Da which indicate cleavage of the molecule into two sections. Biliverdin is the most stable chromophore in our series. Given the same desorption and postionization intensities as used for chlorophyll a, it remains intact during desorption and postionization.

Intensity Dependence. We record the abundance of the intact hemin as a function of the desorption laser intensity I. We see that it can be described by $S = S_0 \cdot I^n$ with n = 1.36 ± 0.13. Similar to other experiments,[4,24] we do not observe any saturation of the desorbed molecular flux in this intensity range.

Fragmentation. Molecular fragmentation may occur chemically during the sample preparation, thermally during desorption[4] or through light-induced processes during postionization. Earlier postionization studies observed substantial fragmentation of hemin, even when the molecule was desorbed into a buffer gas.[25]

In Figure 4 we show that LIAD is intrinsically soft and that all hemin fragments observed in Figure 3 are due to VUV ionization. In Figure 4a we plot the fragment-to-parent ratio as a function of the desorption laser intensity. The fragment ratio remains constant, within 20%, even when we vary the desorption intensity by more than a factor of 60, confirming the softness of the LIAD process. As a function of the detection laser intensity, however, this ratio grows by a factor of 5 and saturates (Figure 4b). This is demonstrated by the hemin spectra at low and high ionization laser intensity in Figure 4c,d.

The situation is different for chlorophyll a, where molecules can lose their side chain even at the lowest ionization intensity required to get a sufficient signal. This indicates that fragmentation most likely occurs during the desorption process.

In an independent experiment we have tested the ionization of hemin at 266 nm and find that this two-photon process leads to substantial fragmentation. This shows that 157.6 nm light provides more efficient ionization than 266 nm, making it better suited to mass spectrometry of biochromophores.

DOI: 10.1021/acs.analchem.5b00601
Anal. Chem. 2015, 87, 5614−5619

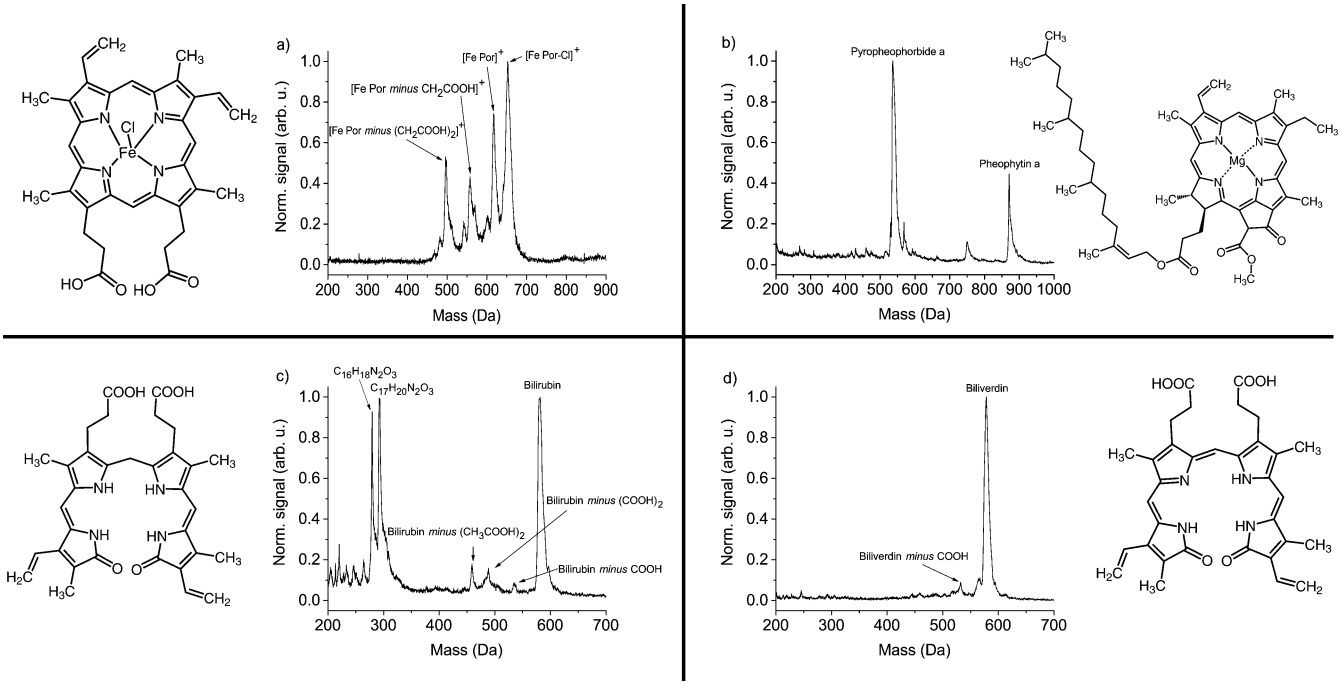

Figure 3. LIAD mass spectra after VUV ionization of (a) hemin, (b) chlorophyll, (c) bilirubin, and (d) biliverdin. Chlorophyll a, bilirubin, and biliverdin were desorbed with Φ_{des} = 54 MW/cm^2, hemin with Φ_{des} = 89 MW/cm^2. The ionization intensity for all molecules was Φ_{ion} = 1.1(1) MW/cm^2.

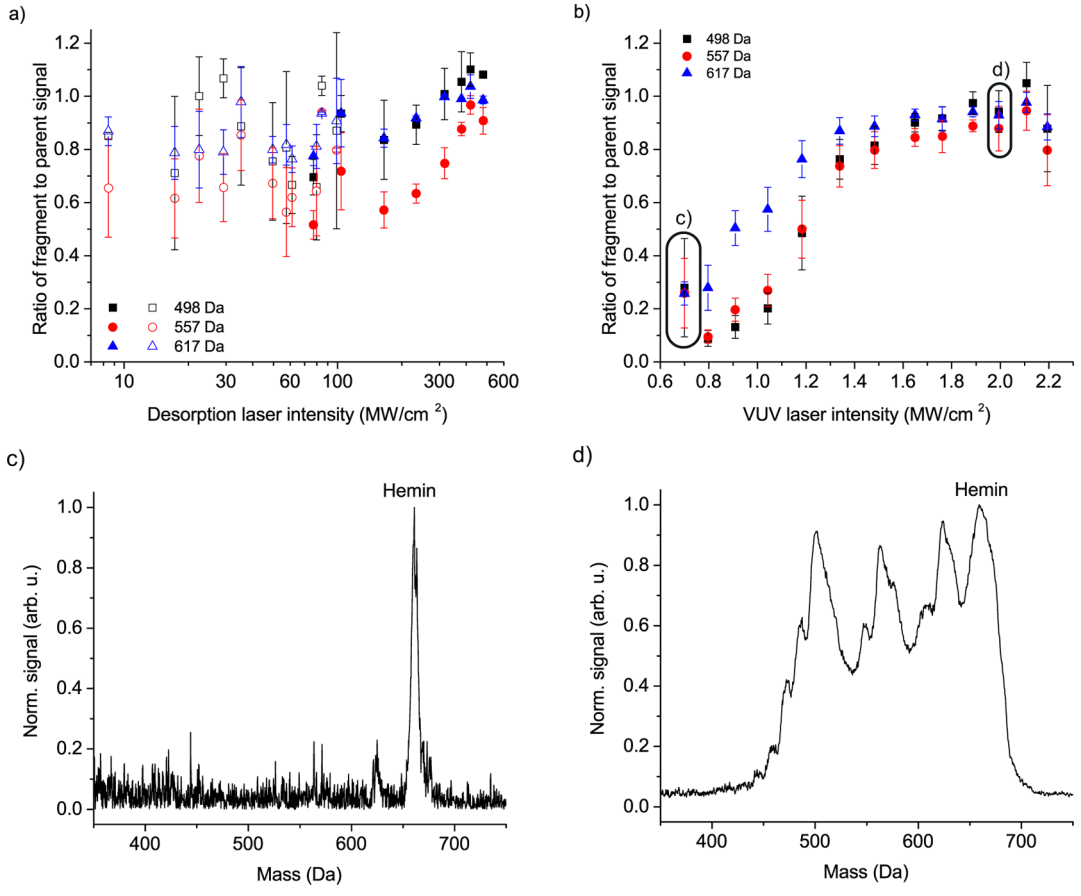

Figure 4. Comparison of LIAD-VUV-TOF-MS for hemin at (a) Φ_{ion} = 0.7(1) MW/cm^2 and (b) Φ_{ion} = 2.0(2) MW/cm^2 reveals that ionization at VUV high intensities leads to fragmentation, while the LIAD process itself is soft.

DOI: 10.1021/acs.analchem.5b00601
Anal. Chem. 2015, 87, 5614−5619

Velocity Distribution. Many applications in physical chemistry require slow particle beams. We therefore characterize the molecular beam velocity after LIAD by counting the number of molecules as a function of the delay between the desorption and the photoionization laser pulses. The resulting distribution is shown in Figure 5. For hemin launched from titanium, we find a most probable velocity of (49 ± 5) m/s and still substantial signal as low as 25 m/s. The error bar in the velocity includes the estimated uncertainty in the desorption time of up to several tens of microseconds.[4,11]

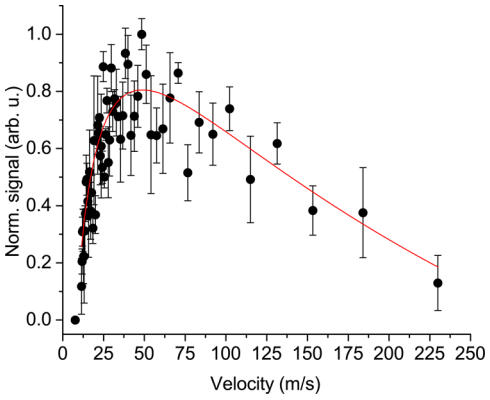

Figure 5. Velocity distribution of neutral hemin released by LIAD from a titanium foil with Φ_{des} = 15 MW/cm^2 and Φ_{ion} =1.3(1) MW/cm^2. Each data point is an average over 30 shots for each of five individual samples. The red line is a guide to the eye. The vertical error bars represent the standard error caused by sample inhomogeneities.

RESULTS: LIBRARIES

Mass Spectra. A typical mass spectrum of **1*Lx*** is shown in Figure 6a. The most abundant molecule contains six perfluoroalkyl side chains and has a mass of approximately 4 550 Da. The peaks are separated by $\Delta m = m_{chain} - m_F$ = 460 Da. Finding m_F in the mass difference corroborates the hypothesis that the observed mass distribution is due to the chemical synthesis. In the case of LIAD-induced fragmentation, the broken bond would not be refluorinated. The same holds true for **2*Lx*** (Figure 6b). Here the peak distance of 763 Da also corresponds to the mass difference between a side chain ($SH_{15}C_{20}F_{26}$) and a fluorine atom.

Mass Dependent Velocities. Earlier experiments[23] showed that thermal beams of **2*Lx*** at T = 500 K had a most probable velocity around 80 m/s. In comparison, Figure 7 shows the mass-dependence of the molecular velocities after LIAD for several porphyrin derivatives, from ZnTPP (m = 678 Da) to functionalized molecules beyond m = 10 000 Da. All were launched from an 8 μm thick tantalum foil.

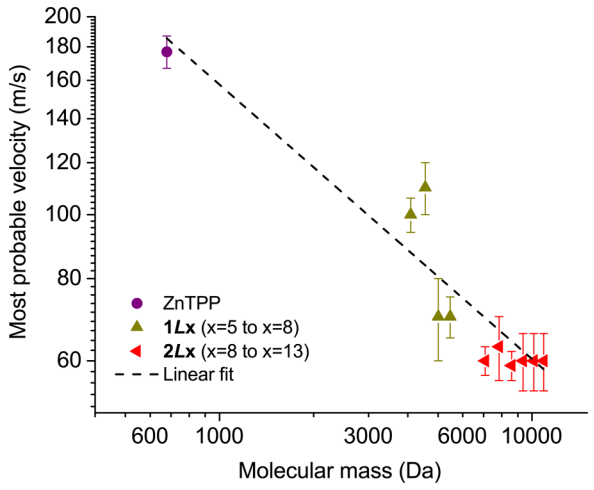

Figure 7. Mass-dependence of the molecular beam velocity after LIAD from tantalum. A linear fit to the double-logarithmic graph yields the power law $v \propto m^{-0.42\pm0.06}$.

A linear fit to the double-logarithmic plot indicates a power law for the mass dependence of the most probably velocity $v \propto m^{-0.42\pm0.06}$. Similar experiments were carried out to determine the initial velocity of ions in MALDI.[27] The authors found a similar power law $v \propto m^{-0.32\pm0.2}$, albeit with particle velocities 10 times larger. A comparison of LIAD with matrix-free direct laser desorption[26] of **2*Lx*** shows that LIAD velocities are generally at least 3 times slower than MALDI.

Substrate Dependence. The choice of foil material also influences the most probable velocity. A comparison of hemin (Figure 5, 49 m/s) with ZnTPP (Figure 7, 177 m/s) shows that LIAD generates 3−5 times slower beams using titanium foils rather than tantalum. A more detailed comparison of LIAD with ZnTPP confirms this material dependency (see Figure 8).

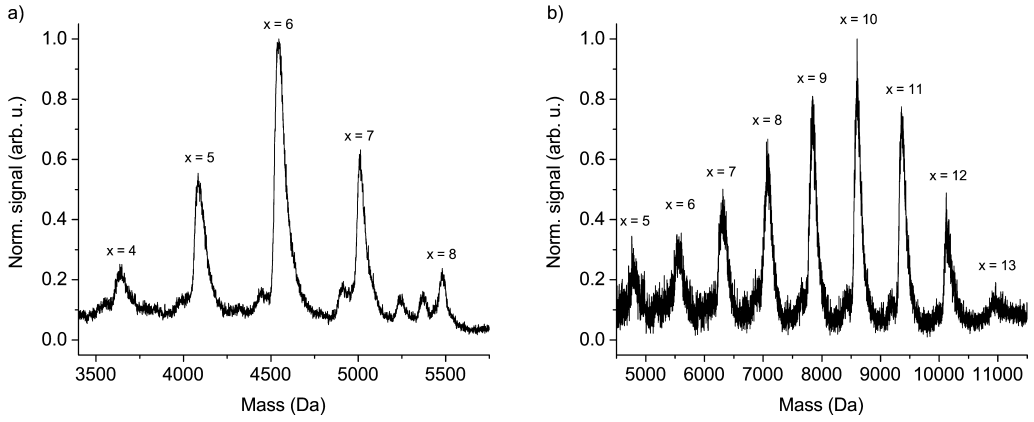

Figure 6. LIAD mass spectrum of the perfluoroalkyl-functionalized porphyrin libraries (a) **1*Lx*** and (b) **2*Lx***. The observed peak separation supports the assumption of fragment-free desorption.[26]

DOI: 10.1021/acs.analchem.5b00601
Anal. Chem. 2015, 87, 5614−5619

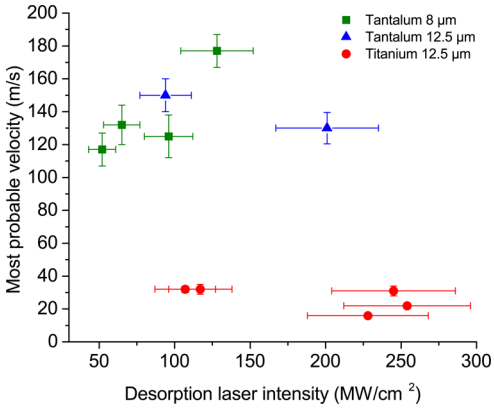

Figure 8. Influence of the foil material, foil thickness, and desorption laser intensity on the most probable velocity of the molecular beam of ZnTPP. Three different foils were used: tantalum (8 and 12.5 μm) and titanium 12.5 μm. The velocity is largely independent from the laser power and the foil thickness in this range. It decreases, however, substantially when we replace tantalum by titanium.

For a given foil material and thickness, different desorption laser intensities change the overall flux but not the beam velocity (Figure 8). This finding is in good agreement with previous studies.[4] In Figure 8 we find no dependence of particle velocity on the foil thickness even though thinner metal sheets are expected to reach higher surface temperatures. Many mechanisms have been suggested to explain this substrate dependence. Zinovev et al.[4] proposed that molecular microcrystals on the sample may not be in their minimal energy state. During the desorption process, these crystals may thus eject the analyte molecules with an excess energy. It depends on the foil and the analyte material and is expected to be higher for tantalum than for titanium. In addition, the desorption laser deforms the foil, forming dimples and bumps on the back and front side of the metal sheet. Finally, substrate particles are coejected in the desorption process.[28] Thus, energy will not only be transferred by heating but also through mechanical stress. The shock-wave induced longitudinal pressure on the surface is larger for tantalum than for titanium. As a result, the velocity of the desorbed molecules is also expected to be higher for tantalum.

CONCLUSION AND OUTLOOK

We have demonstrated that LIAD enables natural biochromophores and massive, functionalized porphyrins to be launched into the gas phase with only minor fragmentation in all cases but one. LIAD can be performed in high vacuum close to the acceptance volume of a mass spectrometer, which is a benefit for analytical chemistry. Single photon postionization at 157.6 nm is a sensitive and specific preparation tool for many molecules below 2000 Da.[29]

In addition, we find that laser-induced acoustic desorption emits very slow molecular beams, which is useful for numerous experiments in chemistry and physics. Long interaction times are important for precision spectroscopy where gains in resolution typically scale with $1/v$. In classical[13,30] and quantum deflectometry,[18] low velocities are even more important as the resolution scales with $1/v^2$.[31] The analyte velocity also determines its de Broglie wavelength in matter-wave interferometers. LIAD of biliverdin or chlorophyll provides beams with $\lambda_{dB} = 2 \times 10^{-11}$ m, i.e., 10 times longer than in typical thermal beams of molecules with a similar mass.[17]

The slow velocities obtained using LIAD are comparable to those realized through electric,[16] magnetic,[32] or mechanical[33] slowing methods. However, slowing has only been demonstrated for atoms and small molecules so far.

Laser desorption into an adiabatically expanding gas jet provides an equally soft method to launch biomolecules[34] and even large amino acid clusters[35] into the gas phase with a narrow velocity distribution. In comparison, LIAD beams are typically 5−10 times slower.

For particles around m = 25 000 Da,[36] we observed velocities as low as 6 m/s in our LIAD experiments. This may one day enable a molecular fountain of neutral molecules. Even lower velocities, v = 1.5 m/s, have been achieved for naphthalene ($C_{10}H_8$) using a cold, effusive buffer gas.[37] Demonstrations with fragile biomolecules have, however, remained a challenge. LIAD is currently the most universal method of generating slow molecular beams of neutral, or low charge, particles which can easily be incorporated into existing analytical instruments.

ASSOCIATED CONTENT

Supporting Information

Synthesis and characterization details of library **1*Lx***. The Supporting Information is available free of charge on the ACS Publications website at DOI: 10.1021/acs.analchem.5b00601.

AUTHOR INFORMATION

Corresponding Author

*E-mail: markus.arndt@univie.ac.at.

Author Contributions

LIAD experiments, U.S., L.W., J.H, and M.A.; chlorophyll preparation, C.G and A.V; synthesis of functionalized biochromophores, L.F., J.T., and M.M; writing, U.S., L.W., and M.A with input by all authors.

Notes

The authors declare no competing financial interest.

ACKNOWLEDGMENTS

Our work has been supported by the European Research Council (Grant 320694), the European Commission (Grant 304886), the Austrian Science Fund (FWF): Grant W1210-3, the Swiss National Science Foundation, as well as the Swiss Nanoscience Institute.

REFERENCES

(1) Tanaka, K.; Waki, H.; Ido, Y.; Akita, S.; Yoshida, Y.; Yoshida, T. *Rapid Commun. Mass Spectrom.* **1988**, *2*, 151−153.
(2) Fenn, J. B.; Mann, M.; Meng, C. K.; Wong, S. F.; Whitehouse, C. M. *Science* **1989**, *246*, 64−71.
(3) Golovlev, V. V.; Allman, S. L.; Garrett, W. R.; Taranenko, N. I.; Chen, C. H. *Appl. Phys. Lett.* **1997**, *71*, 852−854.
(4) Zinovev, A. V.; Veryovkin, I. V.; Moore, J. F.; Pellin, M. J. *Anal. Chem.* **2007**, *79*, 8232−8241.
(5) Vertes, A.; Gijbels, R.; Adams, F. *Laser Ionization Mass Analysis*; Wiley & Sons: New York, 1993; pp 127−175.
(6) Golovlev, V. V.; Allman, S. L.; Garrett, W. R.; Taranenko, N. I.; Chen, C. H. *Int. J. Mass Spectrom. Ion Processes* **1997**, *169−170*, 69−78.
(7) Bald, I.; Dabkowska, I.; Illenberger, E. *Angew. Chem., Int. Ed.* **2008**, *47*, 8518−8520.
(8) Crawford, K. E.; Campbell, J. L.; Fiddler, M. N.; Duan, P.; Qian, K.; Gorbaty, M. L.; Kenttämaa, H. I. *Anal. Chem.* **2005**, *77*, 7916−7923.
(9) Asenbaum, P.; Kuhn, S.; Nimmrichter, S.; Sezer, U.; Arndt, M. *Nat. Commun.* **2013**, *4*, 2743.

DOI: 10.1021/acs.analchem.5b00601
Anal. Chem. 2015, 87, 5614−5619

(10) Peng, W.-P.; Lin, H.-C.; Lin, H.-H.; Chu, M.; Yu, A.; Chang, H.-C.; Chen, C. H. *Angew. Chem., Int. Ed.* **2007**, *46*, 3865−3869.
(11) Calvert, C. R.; et al. *Phys. Chem. Chem. Phys.* **2012**, *14*, 6289−6297.
(12) Chen, J.; Jia, L.; Zhao, L.; Lu, X.; Guo, W.; Weng, J.; Qi, F. *Energy Fuels* **2013**, *27*, 2010−2017.
(13) Bonin, K. D.; Kresin, V. V. *Electric-Dipole Polarizabilities of Atoms, Molecules and Clusters*; World Scientific: Singapore, 1997.
(14) Antoine, R.; Compagnon, I.; Rayane, D.; Broyer, M.; Dugourd, P.; Sommerer, N.; Rossignol, M.; Pippen, D.; Hagemeister, F. C.; Jarrold, M. F. *Anal. Chem.* **2003**, *75*, 5512−5516.
(15) Heiles, S.; Schäfer, R. *Dielectric Properties of Isolated Clusters: Beam Deflection Studies*; Springer Briefs in Molecular Science; Springer: Heidelberg, Germany, 2014.
(16) van de Meerakker, S. Y. T.; Bethlem, H. L.; Vanhaecke, N.; Meijer, G. *Chem. Rev.* **2012**, *112*, 4828−4878.
(17) Juffmann, T.; Ulbricht, H.; Arndt, M. *Rep. Prog. Phys.* **2013**, *76*, 086402.
(18) Arndt, M. *Phys. Today* **2014**, *67*, 30−36.
(19) Shioi, Y. In *Chlorophylls and Bacteriochlorophylls*; Grimm, B., Porra, R. J., Rüdiger, W., Scheer, H., Eds.; Advances in Photosynthesis and Respiration; Springer: Dordrecht, The Netherlands, 2006; Vol. *25*; pp 123−131.
(20) Balaz, M.; Collins, H. A.; Dahlstedt, E.; Anderson, H. L. *Org. Biomol. Chem.* **2009**, *7*, 874−888.
(21) Felix, L.; Sezer, U.; Arndt, M.; Mayor, M. *Eur. J. Org. Chem.* **2014**, 6884−6895.
(22) Tüxen, J.; Eibenberger, S.; Gerlich, S.; Arndt, M.; Mayor, M. *Eur. J. Org. Chem.* **2011**, 4823−4833.
(23) Eibenberger, S.; Gerlich, S.; Arndt, M.; Mayor, M.; Tüxen, J. *Phys. Chem. Chem. Phys.* **2013**, *15*, 14696−14700.
(24) Dow, A. R.; Wittrig, A. M.; Kenttämaa, H. I. *Eur. J. Mass Spectrom.* **2012**, *18*, 77−92.
(25) Ha-Thi, M.-H.; Shafizadeh, N.; Poisson, L.; Soep, B. *Phys. Chem. Chem. Phys.* **2010**, *12*, 14985−14993.
(26) Schmid, P.; Stöhr, F.; Arndt, M.; Tüxen, J.; Mayor, M. *J. Am. Soc. Mass Spectrom.* **2013**, *24*, 602−608.
(27) Tomalová, I.; Frankevich, V.; Zenobi, R. *Int. J. Mass Spectrom.* **2014**, *372*, 51−53.
(28) Lescoute, E.; De Ressguier, T.; Chevalier, J.-M.; Loison, D.; Cuq-Lelandais, J.- P.; Boustie, M.; Breil, J.; Maire, P.-H.; Schurtz, G. *J. Appl. Phys.* **2010**, *108*, 093510.
(29) Hanley, L.; Zimmermann, R. *Anal. Chem.* **2009**, *81*, 4174−4182.
(30) Heer, W. A. D.; Kresin, V. V. In *Handbook of Nanophysics*; Sattler, K. D., Ed.; CRC Press: Singapore, 2011; pp 10/1−26.
(31) Eibenberger, S.; Cheng, X.; Cotter, J. P.; Arndt, M. *Phys. Rev. Lett.* **2014**, *112*, 250402.
(32) Narevicius, E.; Libson, A.; Parthey, C. G.; Chavez, I.; Narevicius, J.; Even, U.; Raizen, M. G. *Phys. Rev. A.* **2008**, *77*, 051401(R).
(33) Gupta, M.; Herschbach, D. R. *J. Phys. Chem. A* **1999**, *103* (50), 10670−10673.
(34) Grotemeyer, J.; Boesl, U.; Walter, K.; Schlag, E. W. *OMS Lett.* **1986**, *21*, 595−597.
(35) Marksteiner, M.; Haslinger, P.; Sclafani, M.; Ulbricht, H.; Arndt, M. *J. Phys. Chem. A* **2009**, *113*, 9952−9957.
(36) Sezer, U.; Schmid, P.; Felix, L.; Mayor, M.; Arndt, M. *J. Mass Spectrom.* **2015**, *50*, 235−239.
(37) Patterson, D.; Tsikata, E.; Doyle, J. M. *Phys. Chem. Chem. Phys.* **2010**, *12*, 9736−9741.

■ NOTE ADDED AFTER ASAP PUBLICATION

This paper published ASAP on May 20, 2015. Figure 3 was corrected and the revised version was reposted on June 2, 2015.

DOI: 10.1021/acs.analchem.5b00601
Anal. Chem. 2015, 87, 5614−5619